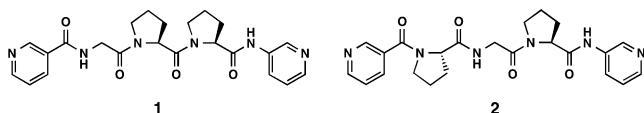


# Peptide [4]Catenane by Folding and Assembly

Tomohisa Sawada,\* Motoya Yamagami, Kazuaki Ohara, Kentaro Yamaguchi, and Makoto Fujita\*

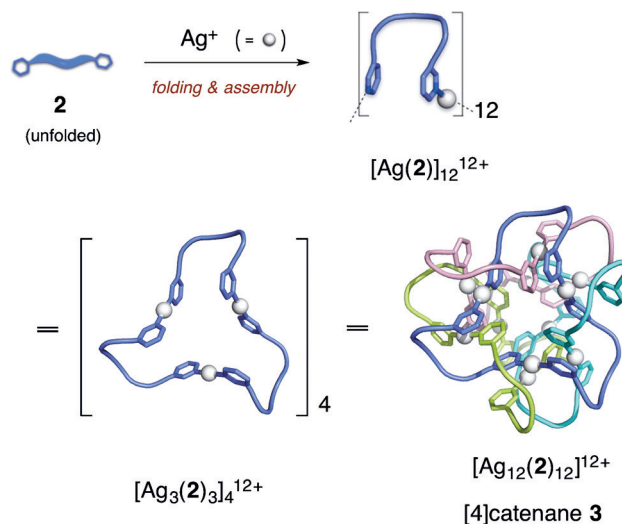
**Abstract:** A topologically complex peptide [4]catenane with the crossing number of 12 was synthesized by a folding and assembly strategy wherein the folding and metal-directed self-assembly of a short peptide fragment occur simultaneously. The latent  $\Omega$ -looped conformation of the Pro-Gly-Pro sequence was found only when pyridines at the C- and N-termini coordinatively bind metal ions ( $\text{Ag}^I$  or  $\text{Au}^I$ ). Crystallographic studies revealed that the  $\Omega$ -looped motifs formed four  $M_3L_3$  macrocycles that were intermolecularly entwined to generate an unprecedented peptide [4]catenane topology.

Interlocked peptide frameworks are often found in the tertiary and quaternary structures of folded proteins.<sup>[1–3]</sup> The formation of such complex molecular topologies in nature arises from multiple weak interactions that intertwine the flexible peptide strands. Both intramolecular (folding) and intermolecular self-assembly (entwining) simultaneously act to generate interlocked peptides. This mechanical stabilization is likely favored, thus leading to their natural selection in molecular evolution. Here we employ a new folding and assembly strategy for constructing robust and well-defined peptide nanostructures from oligopeptides with ditopic metal coordination sites. These peptides are designed such that the addition of metal ions triggers metal-directed self-assembly which simultaneously aids the formation of the dormant  $\Omega$ -loop folding in a synergistic fashion. In our previous study, the Gly-Pro-Pro tripeptide ligand **1** folded into the polyproline II



helix ( $P_{II}$  helix) upon complexation with  $\text{Ag}^I$  ions to form an  $\text{Ag}^I$ -linked  $P_{II}$  helix network.<sup>[4]</sup> Here, the Pro-Gly-Pro ligand **2**, a simple sequence isomer, was found to fold into the  $\Omega$ -looped motif while concomitantly self-assembling into a highly interlocked structure upon metal coordination.

Crystallographic analysis revealed the formation of an unprecedented [4]catenane (**3**), with the crossing number of 12, one of the most complex molecular topologies reported (Scheme 1).



**Scheme 1.** Schematic representation of the self-assembly of  $[\text{Ag}_{12}(\mathbf{2})_{12}]^{12+}$  (**3**) with a topology of a 12-crossing [4]catenane.

The self-assembly of **2** and a  $\text{Ag}^I$  ion was conducted as follows. A three-layered solution was prepared from a methanol solution of **2** (15  $\mu\text{mol}$ /125  $\mu\text{L}$ ; top), a buffer solution (methanol/water = 1:1 (v/v), 200  $\mu\text{L}$ ; middle), and an aqueous solution of  $\text{AgBF}_4$  (15  $\mu\text{mol}$ /125  $\mu\text{L}$ ; bottom) in a capped microtube and kept at 10 °C in an incubator. Upon slow diffusion, high quality single crystals began to grow after two days. The yield of the crystals was 16 % after a two-week incubation, and it increased to 31 % when incubated for nine weeks.

Crystallographic analysis clearly revealed the highly interlocked, discrete molecular structure of **3** assembled from twelve equivalents of **2** ( $\mathbf{3} = [\text{Ag}_{12}(\mathbf{2})_{12}]^{12+}$ ). Each ligand **2** is folded into an  $\Omega$ -loop<sup>[5]</sup> which assembles, through linear silver(I) ions, to form unidirectional  $[\text{N} \rightarrow \text{C Ag}_3(\mathbf{2})_3]$  macrocycles (Figure 1a). Four  $[\text{Ag}_3(\mathbf{2})_3]$  macrocycles are interlocked in such a way that every ring is threaded by the other three (color-coded in Figure 1b). The overall self-assembled structure **3** is thus a dodecanuclear metalloprotein [4]catenane with the crossing number of 12 (Figure 1c,d). The four  $[\text{Ag}_3(\mathbf{2})_3]$  rings, each possessing pseudo- $C_3$  symmetry (Figure 1e), generate the [4]catenane structure **3** in pseudo- $T$ -symmetry with three pseudo- $C_2$  axes and four pseudo- $C_3$  axes.

[\*] Dr. T. Sawada, M. Yamagami, Prof. Dr. M. Fujita  
Department of Applied Chemistry, School of Engineering  
The University of Tokyo  
7-3-1 Hongo, Bunkyo-ku, Tokyo 113-8656 (Japan)  
E-mail: tsawada@appchem.t.u-tokyo.ac.jp  
mfujita@appchem.t.u-tokyo.ac.jp

Dr. K. Ohara, Prof. Dr. K. Yamaguchi  
Faculty of Pharmaceutical Sciences at Kagawa Campus  
Tokushima Bunri University, Sanuki, Kagawa 769-2193 (Japan)

Supporting information for this article can be found under:  
<http://dx.doi.org/10.1002/anie.201600480>.

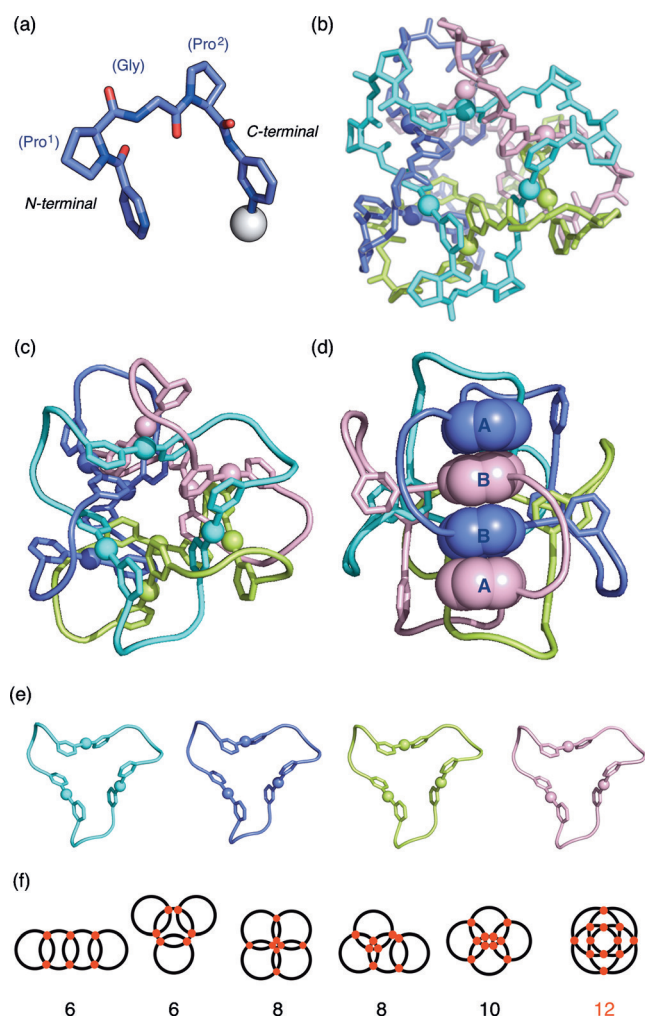


**Figure 1.** Structure of **3**. a) A typical conformation of the peptide ligand **2** observed in the crystal structure. The molecular structure of **3** in b) stick and c) cartoon loop presentations (anions and solvents were omitted for clarity). d) A view looking down a  $C_2$  axis (space-filling presentation emphasizes a tetrameric  $\pi$ -stack). e) Four  $Ag_3(2)_3$  macrocyclic components cut out from the structure of **3**. f) Representative [4]catenane topologies with crossing numbers of 6 to 12.

We note that the crossing number of 12 is the largest possible value of all [4]catenane isomers (Figure 1 f),<sup>[6–8]</sup> and is accordingly one of largest crossing numbers observed<sup>[9]</sup> among reported synthetic interlocked molecules.<sup>[10–13]</sup>

Upon looking down any  $C_2$  axis, two ligands are observed to form a complementary tetrameric  $\pi$ -stack between four pyridines. A representative, color-coded example is provided in Figure 1 d with stacking distances of  $A \cdots B$  and  $B \cdots B$  of 3.92 and 3.66 Å, respectively. This highly symmetrical interdigitated motif likely plays a significant stabilizing role during the assembly of **3**. The  $Ag \cdots Ag$  distances are larger than 5.3 Å, and indicates the absence of direct  $Ag-Ag$  interactions.<sup>[14]</sup> The apical site of  $Ag^I$  is used for coordination of the  $Pro^2$  carbonyl oxygen atom ( $Ag^I \cdots O_{\text{carbonyl}}$  distances: 2.57–2.68 Å), which may slightly stabilize **3** in the solid state though considerably weaker than  $py-Ag^I$  coordination (2.16–2.17 Å).  $BF_4^-$  counter ions effectively fill the voids in the crystals stabilizing the

solid-state structure (see Figure S18 in the Supporting Information).

The preferential folding of **2** into an  $\Omega$ -loop upon metal coordination is favored by the rigidity of two terminal cyclic residues ( $Pro^1$  and  $Pro^2$ ) and flexibility of the central Gly residue, and is likely quite specific to the Pro-Gly-Pro sequence. When similar tripeptide ligands with X-Gly-Pro sequences (**4** and **5** in Figure 2 a, where X is an analogous cyclic amino acid residue) were reacted with  $Ag^I$  ions, an almost superimposable [4]catenane structure, **6**, was formed from **4** ( $6 = [Ag_{12}(4)_{12}]^{12+}$ ; Figure 2 b). However, the ligand **5**, with a piperidine ring as the X residue, did not assemble into a [4]catenane because of the increased flexibility of the X residue.

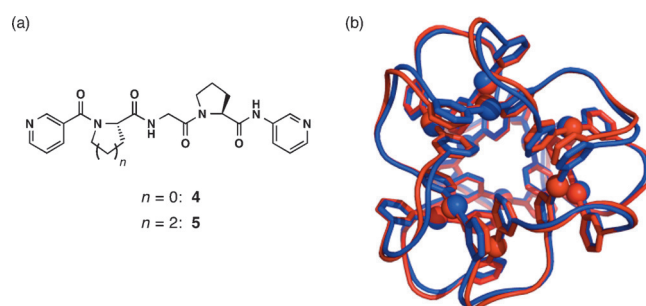


**Figure 2.** Analogous [4]catenane. a) Structure of tripeptides **4** and **5**. b) Overlay of crystal structures **3** (red) and **6** (blue); the latter is formed from **4** by folding and assembly.

ESI-FTICR-MS confirmed the persistence of the  $M_{12}L_{12}$  composition of **3** in solution. Single crystals of **3** were dissolved in nitromethane (**3**: ca. 85  $\mu\text{M}$ ) and the solution was subjected the MS analysis. High-resolution data clearly characterized  $[Ag_{12}(2)_{12}(BF_4)_9]^{3+}$  peaks at  $m/z = 2493$  with adequate intensities (calcd for  $[Ag_{12}(2)_{12}(BF_4)_9]^{3+}$  2493.77276, found 2493.77703; error 1.7 ppm; see Figure S21).

The  $^1H$  NMR chemical shifts of the pyridine protons and amide NH protons of **3** range between  $\delta = 10.6$  and 6.0 ppm with considerable deviations from ordinary values. The observation is indicative of the highly interlocked [4]catenane structure where many protons are shielded inside (Figure 1 b). Sharper and much clearer signals are observed for the  $Au^I$  analogue **3'** and **6** (Figure 3 c,d), probably because the [4]catenane structures are better stabilized by  $Au^I$  coordination and restricted conformation, respectively. In contrast, **3** is in equilibrium with partially unfolded/dissociated structures (Figure 3 b).

The symmetry of the [4]catenanes **3** and **6** dictated from solution NMR spectroscopy needs careful discussion. X-ray crystallography reveals an almost perfect  $T$ -symmetry for the complexes, where all twelve ligands are equivalent, and thus one predicts the observation of a single set of ligand signals for the NMR spectrum of the  $M_{12}L_{12}$  catenane. However, two sets of  $^1H$  NMR signals in a 1:1 ratio are observed for the catenanes **3**, **3'**, and **6** (Figure 3 b–d). The formation of two different conformational or structural isomers for the [4]catenanes in solution is quite unlikely because the 1:1 ratio of the two ligands did not change under all examined conditions [i.e.

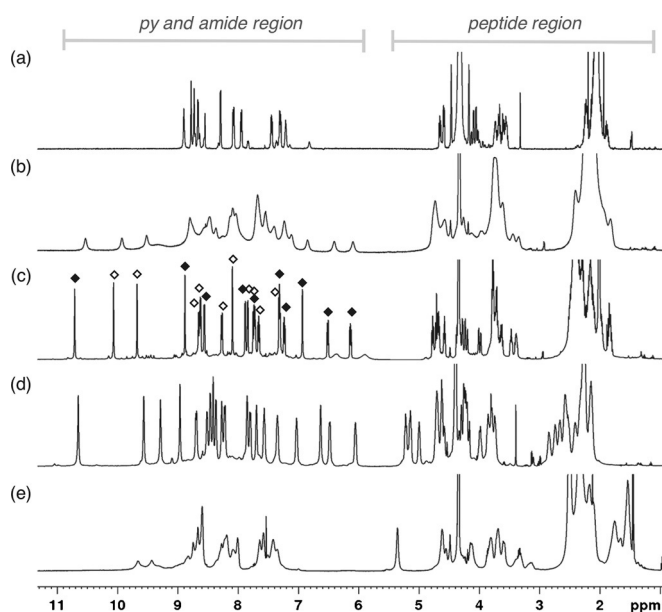


**Figure 3.**  $^1\text{H}$  NMR spectra (500 MHz,  $[\text{D}_3]$ nitromethane): (a) **2** at  $27^\circ\text{C}$ , (b) **3** at  $10^\circ\text{C}$ , (c) **3'** at  $27^\circ\text{C}$ ; two ligands are distinguished by black and white squares. (d) **6** at  $10^\circ\text{C}$ , and (e) **5** +  $\text{AgBF}_4$  at  $10^\circ\text{C}$ ; no [4]catenane formation was observed.

temperature, concentration, metal identity (Ag vs. Au), or ligand (**2** vs. **4**).<sup>[15,16]</sup> Furthermore, the existence of only a single species was clearly indicated by the observation of a single band at  $\log D = -9.5$  in the DOSY NMR spectrum. The  $T$ -symmetry of the [4]catenanes is presumably reduced, in solution, so that twelve ligands are found in two different environments in a 1:1 ratio. We suggest that the cubic lattice circumscribing the  $T$ -symmetric [4]catenanes is deformed into a rhombohedral lattice in solution (Figure 4). After this deformation, four  $C_3$  axes still remain but three  $C_2$  axes are lost. As a result, the two interdigitated,  $\pi$ -stacked ligands,

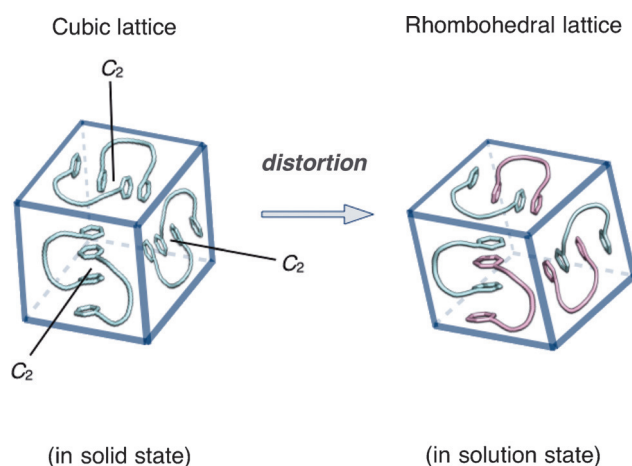


**Figure 4.** Schematic illustration for the distortion of the [4]catenane. In the solid-state (left), the compound has pseudo- $T$ -symmetry enclosed in a cubic lattice, where all the twelve ligands are equivalent. In solution (right), the  $C_2$  axes are lost because of the lattice distortion into rhombohedron. Six interdigitating pairs (see Figure 1 d) are equivalent but each pair contains two inequivalent ligands.

located around every  $C_2$  axis before deformation, become inequivalent. Chemical exchange of the two ligands was observed by ROESY, but the exchange was very slow because the two sets of signals were not coalesced even at  $80^\circ\text{C}$ .

In summary, we prepared highly intertwined metallo-peptide [4]catenanes by a folding and assembly strategy. The crossing number of 12 is one of the largest among reported interlocked synthetic compounds. We emphasize that two orthogonal processes, folding and assembly, are simultaneously combined to obtain highly complex yet symmetrical structures, which are unobtainable by any one individual process. Nature employs this same principle in the formation of interlocked protein structures, such as the HK97 virus capsid<sup>[1a]</sup> and various mysterious knot proteins,<sup>[2]</sup> and continues to inspire researchers in their quest to generate more complex and functional structures through folding and assembly.

## Experimental Section

**Preparation of NMR samples:**  $\text{AgBF}_4$  (25  $\mu\text{mol}$ ) and either the tripeptide ligand **2** or **4** (25  $\mu\text{mol}$ ) were mixed in  $[\text{D}_3]$ nitromethane (0.6 mL) at room temperature. For **3'**,  $[\text{Au}(\text{MeCN})_2]\text{BF}_4$ <sup>[17]</sup> was used. In all cases, self-assembly was completed within 5 min.

**Crystal structure determination:** Crystallographic diffraction data were measured on a Bruker APEX-II/CCD diffractometer or a Bruker Photon 100/CMOS diffractometer equipped with a focusing mirror ( $\text{Mo } K_\alpha$  radiation  $\lambda = 0.71073 \text{ \AA}$ ) with a cryostat system equipped with a  $\text{N}_2$  generator. The crystals were removed from the solution, quickly attached to a loop of nylon fiber with antifreeze reagent (paraton-N, Hampton research), and mounted on a goniometer.

**Crystal data for 3** crystallized from aqueous methanol: Trigonal space group  $R\bar{3}$ ,  $T = 90(2) \text{ K}$ ,  $a = b = 31.270(12) \text{ \AA}$ ,  $c = 44.490(17) \text{ \AA}$ ,  $\alpha = \beta = 90^\circ$ ,  $\gamma = 120^\circ$ ,  $V = 37675(33) \text{ \AA}^3$ ,  $Z = 3$ ,  $\rho_{\text{calcd}} = 1.221 \text{ Mg m}^{-3}$ ,  $F(000) = 41080$ , reflections collected/unique 142729/37970 ( $R_{\text{int}} = 0.1455$ ). The structure was solved by direct methods (SHELXS) and refined by full-matrix least-squares methods (SHELXL) on  $F^2$  with 1569 parameters.  $R_1 = 0.0769$  ( $I > 2\sigma(I)$ ),  $\omega R_2 = 0.1832$ . GOF 0.997, CCDC 1447170 contains the supplementary crystallographic data for this paper. These data can be obtained free of charge from The Cambridge Crystallographic Data Centre.

**Crystal data for 6** crystallized from aqueous methanol: Trigonal space group  $R\bar{3}$ ,  $T = 90(2) \text{ K}$ ,  $a = b = c = 23.2853(8) \text{ \AA}$ ,  $\alpha = \beta = \gamma = 59.69^\circ$ ,  $V = 8864.0(9) \text{ \AA}^3$ ,  $Z = 3$ ,  $\rho_{\text{calcd}} = 1.541 \text{ Mg m}^{-3}$ ,  $F(000) = 4163$ , reflections collected/unique 132549/30749 ( $R_{\text{int}} = 0.1464$ ). 1452 parameters.  $R_1 = 0.0808$  ( $I > 2\sigma(I)$ ),  $\omega R_2 = 0.1576$ . GOF 0.955, CCDC 1447172.

## Acknowledgements

This work was supported by Grants-in-Aid for Specially Promoted Research (24000009), for Young Scientists (A) (15H05481) and Scientific Research on Innovative Areas (26102508).

**Keywords:** macrocycles · peptides · self-assembly · silver · structure elucidation

**How to cite:** *Angew. Chem. Int. Ed.* **2016**, *55*, 4519–4522  
*Angew. Chem.* **2016**, *128*, 4595–4598



- [1] a) W. R. Wikoff, L. Liljas, R. L. Duda, H. Tsuruta, R. W. Hendrix, J. E. Johnson, *Science* **2000**, *289*, 2129–2133; b) Z. Cao, A. W. Roszak, L. J. Gourlay, J. G. Lindsay, N. W. Isaacs, *Structure* **2005**, *13*, 1661–1664; c) D. R. Boutz, D. Cascio, J. Whitelegge, L. J. Perry, T. O. Yeates, *J. Mol. Biol.* **2007**, *368*, 1332–1344.
- [2] a) C. Liang, K. Mislow, *J. Am. Chem. Soc.* **1994**, *116*, 11189–11190; b) F. Takusagawa, S. Kamitori, *J. Am. Chem. Soc.* **1996**, *118*, 8945–8946; c) W. R. Taylor, *Nature* **2000**, *406*, 916–919; d) M. J. Bayro, J. Mukhopadhyay, G. V. T. Swapna, J. Y. Huang, L.-C. Ma, E. Sineva, P. E. Dawson, G. T. Montelione, R. H. Ebright, *J. Am. Chem. Soc.* **2003**, *125*, 12382–12383; e) J. R. Wagner, J. S. Brunzelle, K. T. Forest, R. D. Vierstra, *Nature* **2005**, *438*, 325–331.
- [3] a) T. O. Yeates, T. S. Norcross, N. P. King, *Curr. Opin. Chem. Biol.* **2007**, *11*, 595–603; b) P. Virnau, A. Mallam, S. Jackson, *J. Phys. Condens. Matter* **2011**, *23*, 033101; c) M. Jamroz, W. Niemyska, E. J. Rawdon, A. Stasiak, K. C. Millett, P. Sulkowski, J. I. Sulkowska, *Nucleic Acids Res.* **2015**, *43*, D306–D314.
- [4] T. Sawada, A. Matsumoto, M. Fujita, *Angew. Chem. Int. Ed.* **2014**, *53*, 7228–7232; *Angew. Chem.* **2014**, *126*, 7356–7360.
- [5] Note that  $\Omega$ -loop conformation is defined for more than six residues in general. See: J. S. Fetrow, *FASEB J.* **1995**, *9*, 708–717.
- [6] Possible isomers of [4]catenane were discussed in early work on catenated circular DNA. See: B. Hudson, J. Vinograd, *Nature* **1967**, *216*, 647–652.
- [7] To the best of our knowledge, this is the first example of [4]catenane with the crossing number of 12. See other types of [4]catenane: a) D. B. Amabilino, P. R. Ashton, C. L. Brown, E. Córdova, L. A. Godínez, T. T. Goodnow, A. E. Kaifer, S. P. Newton, M. Pietraszkiewicz, D. Philp, F. M. Raymo, A. S. Reder, M. T. Rutland, A. M. Z. Slawin, N. Spencer, J. F. Stoddart, D. J. Williams, *J. Am. Chem. Soc.* **1995**, *117*, 1271–1293; b) K.-M. Park, S.-Y. Kim, J. Heo, D. Whang, S. Sakamoto, K. Yamaguchi, K. Kim, *J. Am. Chem. Soc.* **2002**, *124*, 2140–2147; c) M. J. Langton, J. D. Matichak, A. L. Thompson, H. L. Anderson, *Chem. Sci.* **2011**, *2*, 1897–1901.
- [8] To date, a mathematical description, Alexander-Briggs notation, is not available for this topology because of the high complexity. In the case of 12-crossing-number links, over 2000 link invariants exist. See: *Handbook of Knot Theory* (Eds.: W. Menasco, M. Thistlethwaite), Elsevier, Amsterdam, **2005**, Chapter 5.
- [9] Examples of the 12-crossing-number molecule: a) F. Bitsch, C. O. Dietrich-Buchecker, A.-K. Khémiss, J.-P. Sauvage, A. Van Dorsselaer, *J. Am. Chem. Soc.* **1991**, *113*, 4023–4025; b) S. P. Black, A. R. Stefankiewicz, M. M. J. Smulders, D. Sattler, C. A. Schalley, J. R. Nitschke, J. K. M. Sanders, *Angew. Chem. Int. Ed.* **2013**, *52*, 5749–5752; *Angew. Chem.* **2013**, *125*, 5861–5864.
- [10] a) R. S. Forgan, J.-P. Sauvage, J. F. Stoddart, *Chem. Rev.* **2011**, *111*, 5434–5464; b) G. Gil-Ramírez, D. A. Leigh, A. J. Stephens, *Angew. Chem. Int. Ed.* **2015**, *54*, 6110–6150; *Angew. Chem.* **2015**, *127*, 6208–6249.
- [11] See seminal works of unique molecular topologies created by metal-directed self-assembly: a) C. O. Dietrich-Buchecker, J.-P. Sauvage, *Angew. Chem. Int. Ed. Engl.* **1989**, *28*, 189–192; *Angew. Chem.* **1989**, *101*, 192–194; b) J.-F. Nierengarten, C. O. Dietrich-Buchecker, J.-P. Sauvage, *J. Am. Chem. Soc.* **1994**, *116*, 375–376; c) M. Fujita, N. Fujita, K. Ogura, K. Yamaguchi, *Nature* **1999**, *400*, 52–55; d) K. S. Chichak, S. J. Cantrill, A. R. Pease, S.-H. Chiu, G. W. V. Cave, J. L. Atwood, J. F. Stoddart, *Science* **2004**, *304*, 1308–1312; e) D. A. Leigh, R. G. Pritchard, A. J. Stephens, *Nat. Chem.* **2014**, *6*, 978–982.
- [12] See also previous examples of proline-based interlocking molecules: a) R. T. S. Lam, A. Belenguer, S. L. Roberts, C. Naumann, T. Jarrosson, S. Otto, J. K. M. Sanders, *Science* **2005**, *308*, 667–669; b) M.-K. Chung, P. S. White, S. J. Lee, M. L. Waters, M. R. Gagné, *J. Am. Chem. Soc.* **2012**, *134*, 11415–11429; c) M.-K. Chung, S. J. Lee, M. L. Waters, M. R. Gagné, *J. Am. Chem. Soc.* **2012**, *134*, 11430–11443.
- [13] Recent examples of metal-linked catenanes from some other groups: a) N. C. Habermehl, M. C. Jennings, C. P. McArdle, F. Mohr, R. J. Puddephatt, *Organometallics* **2005**, *24*, 5004–5014; b) M. Fukuda, R. Sekiya, R. Kuroda, *Angew. Chem. Int. Ed.* **2008**, *47*, 706–710; *Angew. Chem.* **2008**, *120*, 718–722; c) R. Zhu, J. Lübben, B. Dittrich, G. H. Clever, *Angew. Chem. Int. Ed.* **2015**, *54*, 2796–2800; *Angew. Chem.* **2015**, *127*, 2838–2842; d) F. L. Thorp-Greenwood, A. N. Kulak, M. J. Hardie, *Nat. Chem.* **2015**, *7*, 526–531.
- [14] H. Schmidbaur, A. Schier, *Angew. Chem. Int. Ed.* **2015**, *54*, 746–784; *Angew. Chem.* **2015**, *127*, 756–797.
- [15] This sample condition also easily afforded single crystals of the [4]catenane **3** after a one-day incubation at 10°C. See the crystal structure derived from nitromethane solution in the Supporting Information.
- [16] Total energy of the conformational isomer was estimated, by molecular mechanics calculations, to be larger than that of **3**. See Figure S31 in the Supporting Information.
- [17] K. D. Shimizu, J. Rebek, Jr., *Proc. Natl. Acad. Sci. USA* **1996**, *93*, 4257–4260.

Received: January 16, 2016

Published online: March 3, 2016